



Efficient Radio Frequency Inductive Discharges in Near Atmospheric Pressure Using Immittance Conversion Topology

RAZZAK M. Abdur, TAKAMURA Shuichi, UESUGI Yoshihiko¹⁾ and OHNO Noriyasu²⁾

*Department of Energy Engineering and Science, Graduate School of Engineering,
Nagoya University, Furo-cho, Chikusa-ku, Nagoya 464-8603, Japan*

*¹⁾Department of Electrical and Electronic Engineering, Faculty of Engineering,
Kanazawa University, 2-40-20 Kodatsuno, Ishikawa 920-8667, Japan*

*²⁾EcoTopia Science Institute, Nagoya University,
Furo-cho, Chikusa-ku, Nagoya 464-8603, Japan*

(Received 25 November 2004 / Accepted 10 February 2005)

A radio frequency (rf) inductive discharge in atmospheric pressure range requires high voltage in the initial startup phase and high power during the steady state sustainment phase. It is, therefore, necessary to inject high rf power into the plasma ensuring the maximum use of the power source, especially where the rf power is limited. In order to inject the maximum possible rf power into the plasma with a moderate rf power source of few kilowatts range, we employ the immittance conversion topology by converting a constant voltage source into a constant current source to generate efficient rf discharge by inductively coupled plasma (ICP) technique at a gas pressure with up to one atmosphere in argon. A novel T-LCL immittance circuit is designed for constant-current high-power operation, which is practically very important in the high-frequency range, to provide high effective rf power to the plasma. The immittance conversion system combines the static induction transistor (SIT)-based radio frequency (rf) high-power inverter circuit and the immittance conversion elements including the rf induction coil. The basic properties of the immittance circuit are studied by numerical analysis and verified the results by experimental measurements with the inductive plasma as a load at a relatively high rf power of about 4 kW. The performances of the immittance circuit are also evaluated and compared with that of the conventional series resonance circuit in high-pressure induction plasma generation. The experimental results reveal that the immittance conversion circuit confirms injecting higher effective rf power into the plasma as much as three times than that of the series resonance circuit under the same operating conditions and same dc supply voltage to the inverter, thereby enhancing the plasma heating efficiency to generate efficient rf inductive discharges.

Keywords:

immittance conversion topology, inductively coupled plasma, radio frequency, E-H mode transition, static induction transistor, atmospheric pressure

1. Introduction

Inductively coupled plasma (ICP) technique is one of the methods to generate high-pressure radio frequency (rf) discharges. The concept of ICPs are not new and their generation [1-3], modelling [4,5], characterization [6,7], processing [8,9] and applications [10,11] have been reported in many literatures since the last few decades with the intention of achieving each goal. Although the idea of induction heating was first introduced by Hittorf in 1884 [1], the full concept of induction plasmas and their applications were reported by Reed in 1961 [2,3], and after that a lot of works were conducted by the scientists and researchers all over the world to provide these plasma reactors in the several fields of applications. But, most of these researches were

conducted for low-pressure ICPs, since the initiation and generation of low-pressure ICPs require low-voltage and low-power with their simple and easy diagnostics technique. However, there has been increasing the interest in the potentiality of high-pressure (near atmospheric pressure range) induction plasmas during the past decades in a diversity of researches because of their high-temperature and high-reaction activity, and wide range of applications such as material processing, spray coating of metals and ceramics, thin films deposition, waste materials destruction, and disposal of harmful gases (NO_x, CO₂, O₃, CFC etc.) that are responsible for global warming and environmental pollution. But, high rf voltage and high rf power are the most important requirements for the generation and sustainment of high-

author's e-mail: razzak@ees.nagoya-u.ac.jp

This article is based on the invited talk at the 21st JSPF Annual Meeting (Shizuoka 2004)

pressure (near atmospheric pressure) radio frequency discharges [11]. And because of high-efficiency and high-power operation, high-power semiconductor devices, such as static induction transistor (SIT) inverter power source has become popular in the last decade due to their applications to various kinds of induction heating and plasma generation [12–18]. But, at high operating frequencies in the MHz range, rf system shows transient and strongly dynamic behavior due to the presence of reactive components in the power source [19], and non-linear coupling and dynamic interaction between the plasma and the rf source [20,21]. Inherent problems are, therefore, observed in the radio frequency (rf) power source during high-pressure induction plasma generation [22,23].

During the generation of rf inductive discharges using the conventional series resonance circuit [18], initially an electrostatic discharge (E discharge) develops by the strong axial electrostatic field (100–200 kV/m in atmospheric pressure) due to the high rf voltage on the induction coil for several hundred microseconds, and then a rapid transition from electrostatic to electromagnetic mode occurs after developing the electromagnetic discharge (H discharge) due to induced electric field to form the volumetric induction plasmas [20,21]. A rapid increase of the coil loading resistance and decrease of the effective coil inductance are observed during the mode transition period of the generated plasmas. The loading resistance in the E mode is very small due to a weak coupling between the plasma and rf source, and becomes high in the H mode due to the growth of the inductive plasma. The rf coil current, therefore, drops abruptly when the load changes from the E to H mode due to the resistance rise. The rf coil current also decreases due to plasma reaction by the induction current flows in the azimuthal direction but opposite to that of the rf coil current, which decreases the induced flux. Therefore, the effective coil loading inductance and hence the reactance decreases in the H mode. As a result, the frequency and phase are shifted from their resonance value during the H mode by a value of about 30 kHz and $+\pi/6$ radian, respectively with a driving frequency of 1.2 MHz at atmospheric pressure [22].

Therefore, the total load, which is resistive without plasma due to a resonance tuning becomes slightly inductive in the E mode and slightly capacitive during the H mode, thereby increasing the switching losses of the SIT inverter elements present in the rf system. Hence the inverter output strongly deteriorates, thereby decreasing the dc-rf power conversion efficiency of the rf power source by a value of about 30–40% [22,23]. To overcome these problems, in this paper, a novel immittance conversion circuit is designed for constant-current high-power operation in the high-frequency (MHz) range and employed successfully to enhance the power as well as heating efficiency, thereby generating efficient rf inductive discharges at near atmospheric pressure range in argon.

2. Immittance Circuit

In recent years, the immittance conversion topology [19] has become attractive as a novel power conversion strategy because of its features that a constant voltage source is converted to a constant current source and vice versa. The immittance converter is a combined word of the impedance-admittance converter. In this converter, the output current is proportional to the input voltage and the input current is proportional to the output voltage. A typical T-LCL type immittance circuit employed in the present experiment is sketched in Fig. 1. The immittance conversion system combines the static induction transistor (SIT)-based radio frequency (rf) high-power inverter circuit and the immittance conversion elements including the rf induction coil. The rating of the SIT inverter power source is about 20 kW maximum in pulse operation and 14 kW in continuous operation in a frequency range of 0.2–1.7 MHz.

Since the inductive plasma behaves as a non-linear load due to the dynamic interaction between plasma and rf source [20–22], it is, therefore, necessary to design an ideal immittance circuit in order to apply to such a time-varying inductive plasma load. To determine the circuit elements, we employ the overall resonance condition to the RLC input and output circuit. The design procedure is practically very important in this frequency range, which is described below.

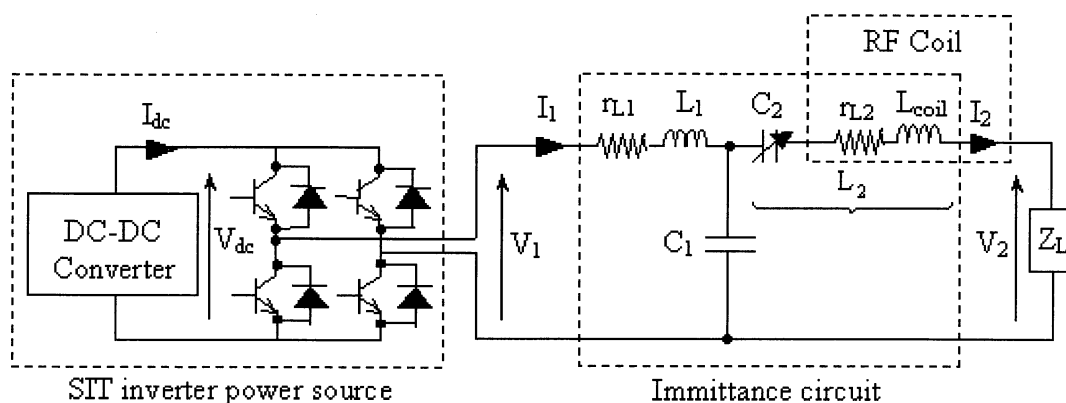


Fig. 1 Equivalent circuit of the combined system consisting of static induction transistor (SIT) inverter unit (one of the six inverter units is shown in the figure) and T-LCL immittance circuit (including rf induction coil) for constant current operation.

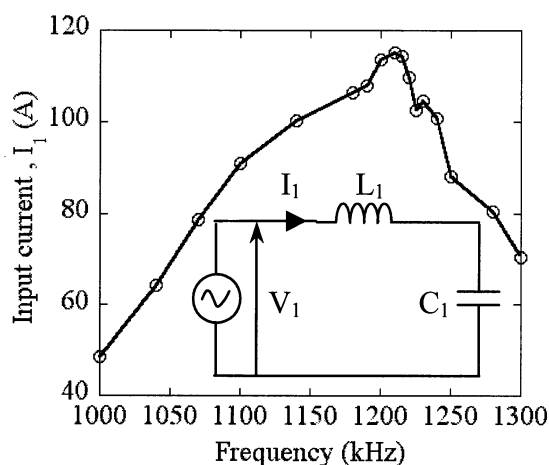


Fig. 2 Driving frequency vs. input current to determine the resonance frequency.

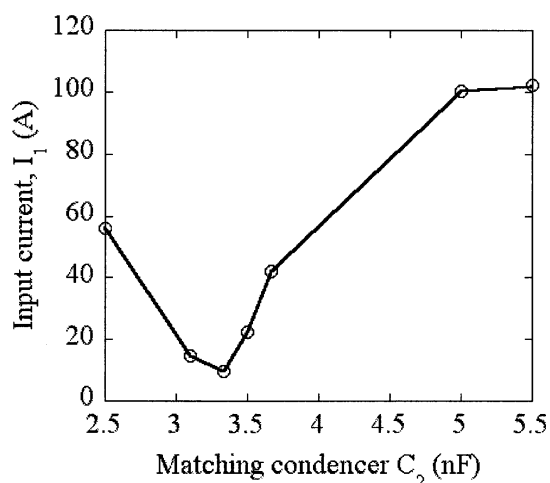


Fig. 3 Input current as a function of matching condenser to determine the optimum value of the matching condenser.

2.1 Determining the resonance frequency

From Fig. 1, the basic voltage-current relation can be written as

$$V_1 = \left(r_{L_1} + j\omega L_1 + \frac{1}{j\omega C_1} \right) I_1 - \frac{1}{j\omega C_1} I_2, \quad (1)$$

$$V_2 = \frac{1}{j\omega C_1} I_1 - \left(r_{L_2} + j\omega L_2 + \frac{1}{j\omega C_1} \right) I_2, \quad (2)$$

$$V_2 = Z_L I_2, \quad (3)$$

where ω is the driving angular frequency and $Z_L (= R_L + jX_L)$ is the plasma loading impedance, which is consisting of a reactive part X_L in addition to a resistive component R_L because the effective coil inductance could change due to the plasma reactor. In Eq. (2) the inductance L_2 is given by

$$L_2 = L_{\text{coil}} - \frac{1}{\omega^2 C_2}, \quad (4)$$

where, L_{coil} is the rf coil inductance and C_2 is the matching condenser to have a reasonable value of L_2 since L_{coil} is determined from the plasma coupling.

In order to find the resonance frequency, resonance condition (maximum power transfer) is applied to the input rf circuit of Fig. 1, which is drawn as an insertion in Fig. 2. Figure 2 shows the input current as a function of frequency by taking the value of $C_1 = 50 \times 10^{-9}$ F. According to maximum power transfer condition, the resonance frequency will be known when the current reaches to its maximum value. From Fig. 2 the resonance frequency is found to be 1.21×10^6 Hz.

2.2 Calculating the primary coil inductance L_1

Applying the resonance condition in the input rf circuit of Fig. 1, which is drawn as an insertion in Fig. 2, it is possible to find the primary coil inductance, which is given by

$$L_1 = \frac{1}{\omega^2 C_1}. \quad (5)$$

Now we know the value of C_1 and the resonance frequency, which are equal to 50×10^{-9} F and 1.21×10^6 Hz, respectively. Therefore, the primary coil inductance calculated by Eq. (5) is about 0.346×10^{-6} H.

2.3 Determining the matching condenser C_2

By including the matching condenser C_2 in the immittance circuit as shown in Fig. 1, the value of output current will be decreased, and we can choose the appropriate value of C_2 when the input current reaches to its minimum value since the output current will be reached to a maximum at that time. Figure 3 shows the input current I_1 as a function of the matching condenser C_2 without plasma, and from Fig. 3 the optimum value of C_2 is found to be about 3.33×10^{-9} F.

2.4 Calculating the value of coil inductance L_{coil}

Using Eqs. (1)–(5), assuming r_{L_1} and r_{L_2} negligible, the relation between V_1 and I_1 can be written as

$$I_1 = (\omega C_1)^2 \left[Z_L + j \left(\omega L_{\text{coil}} - \frac{1}{\omega C_2} - \frac{1}{\omega C_1} \right) \right] V_1. \quad (6)$$

For the resonance condition without plasma, the summation of the last three terms of Eq. (6) must be equal to zero, which gives

$$\omega L_{\text{coil}} - \frac{1}{\omega C_2} - \frac{1}{\omega C_1} = 0. \quad (7)$$

Using Eqs. (5) and (7), the coil inductance is given by

$$L_{\text{coil}} = L_1 + \frac{1}{\omega^2 C_2}. \quad (8)$$

Now we know the values of ω , L_1 and C_2 and using those values the coil inductance calculated by Eq. (8) is found to be about 5.53×10^{-6} H. From Eqs. (4) and (8) we find

$$L_1 = L_2, \tag{9}$$

which is one of the necessary conditions that must be satisfied for the design of an ideal immittance circuit.

2.5 Determining the final driving frequency

The overall operating frequency is determined by the minimum input current without plasma as shown in Fig. 4, which confirms the resonance condition (maximum power transfer). From Fig. 4, the driving frequency is found to be about 1.185×10^6 Hz.

Therefore, by choosing the value of C_1 as 50 nF, the values of L_1 , L_{coil} and C_2 is found to be 0.34 μH , 5.53 μH and 3.33 nF, respectively, and according to Eq. (9) the value of L_2 is obviously 0.34 μH . The overall driving frequency is found to be about 1.2 MHz.

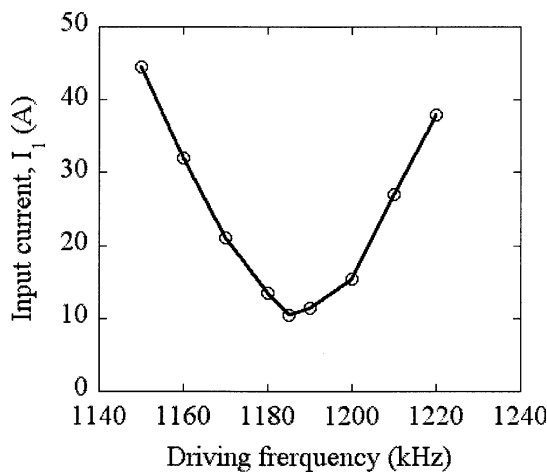


Fig. 4 Input current as a function of frequency to determine the overall driving frequency.

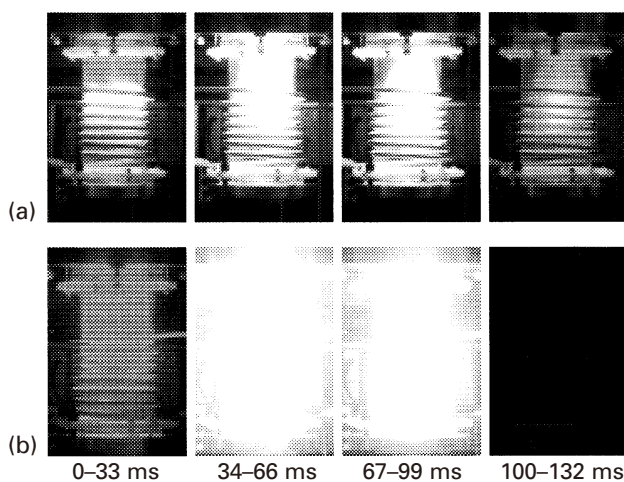


Fig. 5 A series of typical CCD camera pictures with an exposure time of 33 ms, using conventional series resonance circuit (a) and immittance circuit (b). The injected rf power is about 1.2 kW in the case of series resonance circuit (Fig. a), and about 3.0 kW in the case of immittance circuit (Fig. b).

3. Application to Plasma Generation

The immittance circuit designed in the above section, cascading with a static induction transistor (SIT) inverter power source, is employed to generate radio frequency discharges by inductively coupled plasma (ICP) technique in near atmospheric pressure. The maximum output power and frequency rating of the SIT inverter is 20 kW (pulse operation) and 1.7 MHz, respectively. The inverter DC input

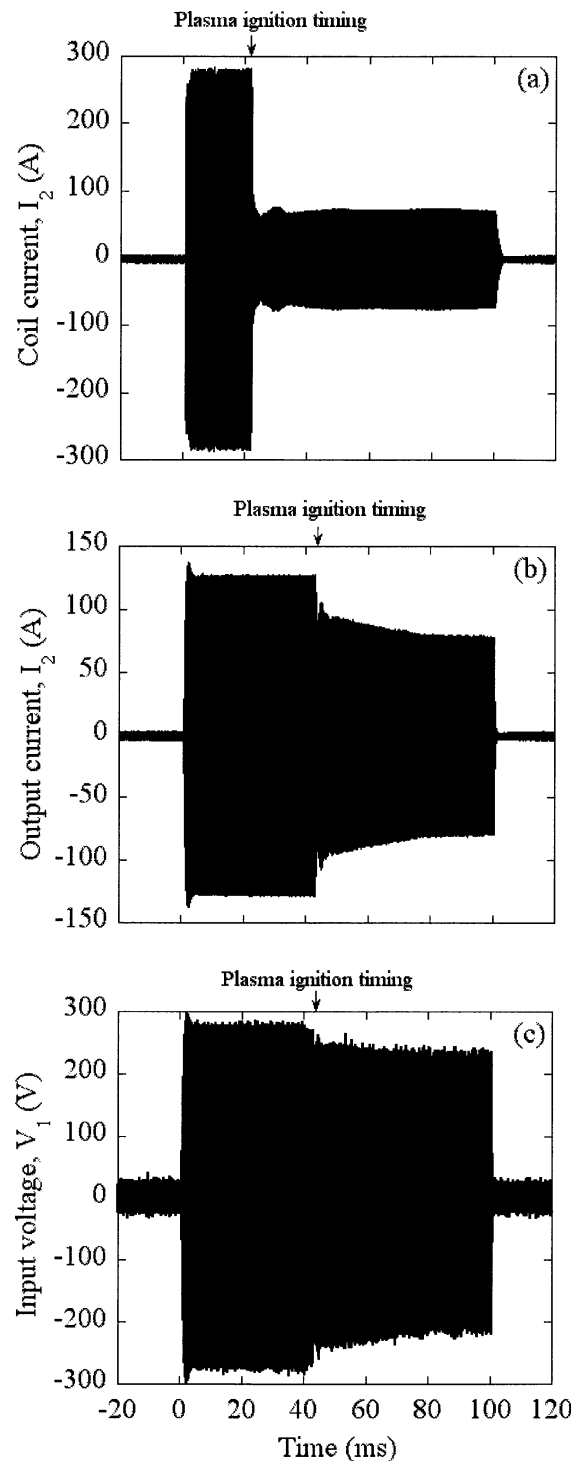


Fig. 6 RF coil current waveform with series resonance circuit (a), and output current (b), and input voltage waveform (c) for immittance circuit during plasma generation.

voltage and current, rf output voltage and current, and rf coil current are measured to analyze the performance of the immittance circuit. The plasmas are sustained in a Pyrex glass tube with an inner diameter of 7 cm and a length of 20 cm. An induction coil consisting of a 7-turn copper tube of 1/4 inches outer diameter is used for the discharge to be occurred. Argon gas with a neutral pressure with up to one atmosphere and a flow rate of 20 lpm is injected both axially and spirally into the discharge chamber. The neutral gas pressure, which is controlled by using a mechanical rotary pump, is measured with a total pressure gauge. The rf power level, which is limited by the cooling capability of the system, is modulated with a 100 ms square wave pulse without applying any cooling system. Repetitive spark discharge, using the spark discharge technique [15,18], with a repetition frequency of 500 Hz for 20 ms (10 pulse with a duration of 2 ms each), is applied simultaneously with the rf pulse to initiate the discharge. A typical automobile spark plug placed at the center of the top flange of the discharge chamber, with a high-voltage transformer circuit, is employed for this purpose. To observe the visible emission of rf discharges, a series of CCD camera pictures with a frame speed of 30 fps are taken by setting the camera perpendicular to the discharge axis.

A series of typical CCD camera pictures of rf inductive discharges at a gas pressure of one atmosphere are presented in Fig. 5. Figure 5(a) represents the discharges generated by conventional series resonance circuit while 5(b) represents the discharges generated by using immittance circuit. It is noticed that with the same operating conditions and same dc voltage supply to the SIT inverter, immittance circuit injected higher effective rf power (about 3.0 kW) to the plasma than that of the series resonance circuit (about 1.2 kW), thereby enhancing the plasma heating efficiency, which helps to generate efficient rf inductive discharges. The comparison of power efficiency using immittance circuit with that of the conventional series resonance circuit will be shown later in Sec. 5.

Figures 6(a) and (b) show rf coil current waveforms during plasma generation with series resonance circuit and immittance circuit, respectively. Fig. 6(a) shows that, with the conventional series resonance circuit, rf coil current drops abruptly by a value of about 75% after the plasma generation due to the impedance rise. However, on the other hand, using the immittance conversion circuit, although the rf coil current drops (about 25%) due to a deviation from ideal immittance circuit and a decrease of the inverter output voltage as shown in Fig. 6(c), but still is much higher than in the case of series resonance circuit. This high rf coil current confirms higher effective rf power injecting into the plasma thereby increasing the dc-rf conversion efficiency [15], and also the effective rf power absorbed by the plasma. Another point has to be mentioned that the starting current [18] is lower in the case of immittance circuit (125 A) than that of the series resonance circuit (275 A) due to the current limit of the immittance circuit as shown in Figs. 6(a) and (b). For this reason, the initial ignition time is much longer in the case of immittance

circuit than that of the conventional RLC series resonance circuit as shown in Fig. 6. This is one of the disadvantages of the immittance conversion circuit over the series resonance circuit. Comparing Figs. 6(a) and (b), it is seen that the ignition starts just about 20 ms after applying the radio frequency power in the case of series resonance circuit while about 40 ms in the case of immittance circuit.

4. Evaluation of Immittance Circuit Properties with Inductive Plasma Load

Before going to evaluate the properties of the immittance circuit with high-pressure rf inductive plasma load, it is necessary to characterize the immittance circuit properties by circuit analysis. Using Eqs. (1)–(3) the voltage to current ratios can be written as

$$\frac{V_1}{I_1} = \left[r_{L_1} + \left(\frac{1}{\omega C_1} \right)^2 \frac{R}{R^2 + X_2^2} \right] + j \left[X_1 - \left(\frac{1}{\omega C_1} \right)^2 \frac{X_2}{R^2 + X_2^2} \right], \quad (10)$$

$$\frac{V_1}{I_2} = \left[-\omega C_1 (r_{L_1} X_2 + R X_1) \right] + j \left[\omega C_1 (r_{L_1} R - X_1 X_2) + \left(\frac{1}{\omega C_1} \right) \right], \quad (11)$$

where $X_1 = \left(\omega L_1 - \frac{1}{\omega C_1} \right)$, $X_2 = \left(X_L + \omega L_2 - \frac{1}{\omega C_1} \right)$ and $R = R_L + r_{L_2}$.

Applying the resonance condition ($X_1 = 0$ and $X_2 = X_L$) and assuming that the internal resistances of the inductors are negligible ($r_{L_1} = r_{L_2} = 0$), Eqs. (10) and (11) become

$$\frac{V_1}{I_1} = \frac{Z_0^2}{Z_L}, \quad (13)$$

$$\frac{V_1}{I_2} = j Z_0, \quad (14)$$

respectively, where Z_0 is the characteristic impedance given by

$$Z_0 = \sqrt{L_1/C_1}. \quad (15)$$

Also Eq. (13) can be rewritten as

$$\frac{V_1}{I_1} = R_s + j X_s = \frac{Z_0^2}{R_L + j X_L},$$

which gives

$$R_s = \frac{Z_0^2 R_L}{R_L^2 + X_L^2}, \quad X_s = -\frac{Z_0^2 X_L}{R_L^2 + X_L^2}. \quad (16)$$

Using Eqs. (13) and (14), the properties of the immittance circuit can be characterized by the following F-matrix

$$\begin{bmatrix} V_1 \\ I_1 \end{bmatrix} = \begin{bmatrix} 0 & Z_0^2 \\ jZ_0 & 0 \end{bmatrix} \begin{bmatrix} V_2 \\ I_2 \end{bmatrix}. \quad (17)$$

From Eq. (16) it is seen that the value of R_s and X_s depends on the plasma loading resistance R_L and reactance X_L since the characteristic impedance Z_0 is a constant. The value of R_s and X_s calculated from the waveform of V_1 and I_1 (Fig. 6) are plotted in Fig. 7, from where it is seen that R_s is large (about 22 Ω) before the plasma ignition due to the small loading impedance without plasma, and decreases after the plasma ignition (about 1.75 – 2.5 Ω) due to the gradual increase of plasma loading impedance. It is also seen that the value of X_s is relatively large and positive (about +0.75 Ω) during E discharge mode due to small loading reactance for the weak capacitive coupling of streamer-like electrostatic discharge [20,21], and decreases and becomes slightly negative (about -0.25 to -1.0 Ω) after the plasma generation. This is because with the high rf coil current supplied by the immittance circuit, the induced azimuthal current and thus the induced flux inside the plasma increases, which decreases the original axial magnetic flux and thus the effective coil loading inductance or the loading reactance. Therefore, the total load behaves as slightly capacitive with the high rf coil current using the immittance circuit. Now, the value of R_s and X_s calculated from the plasma loading resistance R_L and reactance X_L using Eq. (16) are found to be about 2.5 Ω and -0.65 Ω respectively after the plasma generation, which shows a good agreement with the results shown in Fig. 7 that are calculated from the waveform of V_1 and I_1 (Fig. 6). These agreements confirm a good design of T-LCL immittance circuit in the high-frequency (MHz) range for high-power induction plasma generation.

From Eq. (14) it is seen that the ratio $|V_1/I_2|$ should be a constant value both in magnitude and phase, which are equal to Z_0 ohm and $+\pi/2$ radian, respectively. This shows that the output current of the immittance circuit remains constant regardless of the loading impedance provided that the input voltage is fixed. Figure 8 shows the comparison of the characteristic impedance Z_0 calculated by circuit elements, which is about 2.63 Ω in the present design, with that of the experimental result evaluated from the waveform of V_1 and I_2 (Fig. 6). It is seen that the calculated results agree well with that of the experimental one, which also confirms a good design of constant current, high-power immittance circuit for the generation of high-pressure rf inductive discharges. However, from Fig. 8 it is seen that the estimated value of $|V_1/I_2|$ has a slight deviation after the plasma ignition. This discrepancy probably comes from the effect of the internal resistances of the primary inductor and that of the rf induction coil, which are assumed to be zero in the above calculations [Eqs. (13)–(17)] for an ideal immittance circuit. But, since the internal resistance of the rf coil will automatically be included with the plasma resistance, we will here, therefore, discuss the influence of internal resistance of the primary

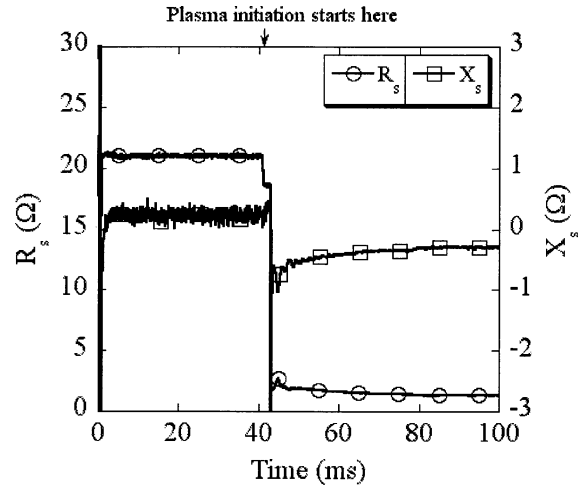


Fig. 7 Evaluation of the immittance circuit properties using equation (13). Comparison between circuit calculation and experimental results.

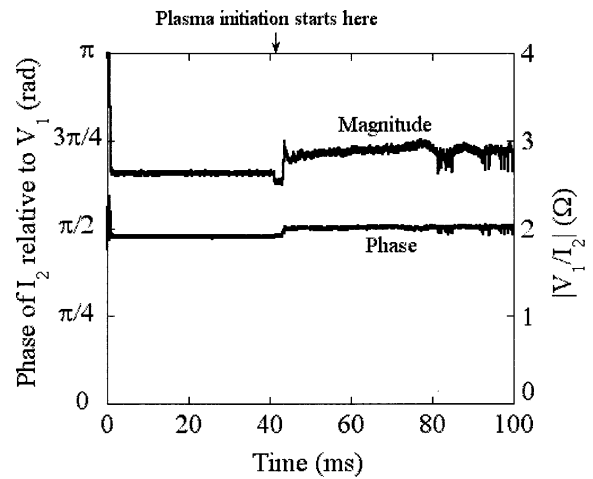


Fig. 8 Evaluation of the immittance circuit properties. Comparison between circuit calculation and experimental results.

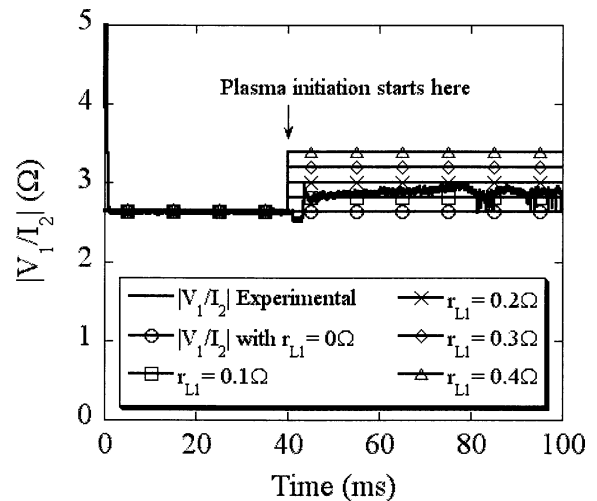


Fig. 9 Effect of internal resistance of the primary inductor on the V_1/I_2 ratio. Comparison of calculation with that of the experimental results. The value of plasma loading resistance R_L before and after the plasma generation is 0.2 Ω and 5 Ω , respectively.

inductor only.

Figure 9 shows the effect of internal resistance of the inductor in the primary side in which the calculated results are compared with that of the experimental one. It is observed that with the internal resistance $r_{L1} = 0$, the ratio $|V_1/I_2|$ remains constant before and after the plasma generation, but the ratio $|V_1/I_2|$ increases with increasing the internal resistance after the plasma generation. Therefore, the discrepancy between experimental result and calculation seen in Fig. 8 comes from the effect of the internal resistance of the primary inductor, and from Fig. 9, the internal resistance of the primary inductor that matches with the experimental result is found to be about 0.15Ω .

5. Enhancing the Power Efficiency

The time evolution of effective rf power using the immittance circuit with that of the series resonance circuit is compared in Fig. 10(a), from where the value of effective rf power, calculated from the rf power supply side, is found to

be about 3 kW with immittance circuit, while about 1.2 kW with series resonance circuit after the plasma ignition under the same operating condition. Therefore, the effective rf power injected into the plasma is about three times using immittance circuit than that of the series resonance circuit after the plasma ignition. Figure 10(b) shows the comparison of dc-rf power conversion efficiency (ratio of rf power and dc power) using immittance circuit with that of the conventional series resonance circuit, from where it is seen that the power conversion efficiency is about 90–92% using the immittance circuit, which is as much as three times than that of the conventional series resonance circuit (which is about 30%). Because, using the series resonance circuit, the total load behaves slightly capacitive due to the positive phase shift (about $+\pi/6$ radian) after the plasma generation, which increases the switching losses of the SIT inverter elements, thereby decreasing the rf output power and thus the dc-rf conversion efficiency [22]. On the other hand, having the constant coil current properties as shown in Fig. 8, the immittance circuit helps to inject high rf power into the plasma thereby increasing the plasma heating as well as the plasma production efficiency.

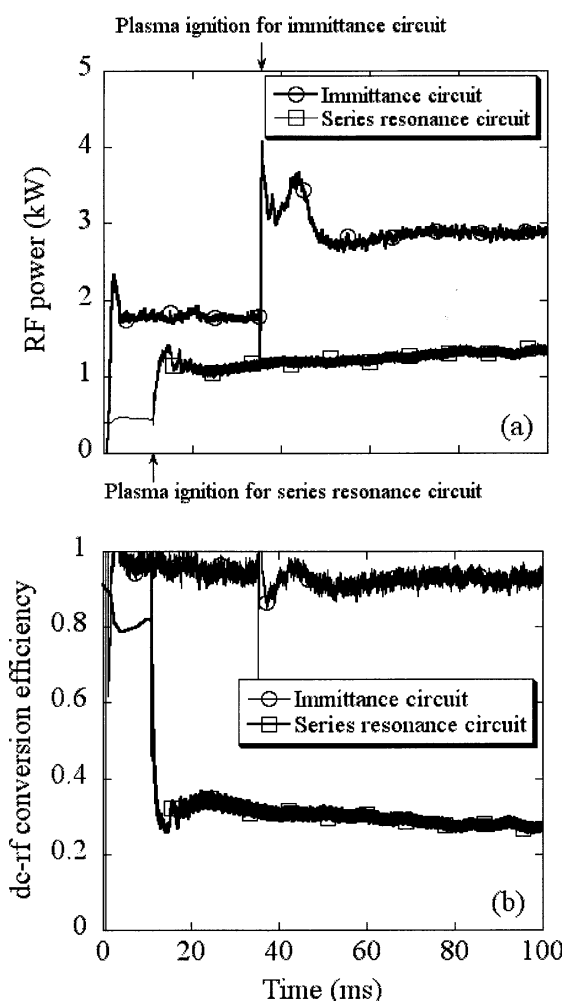


Fig. 10 Comparison of the performance of immittance circuit with that of the conventional series resonance circuit in high-pressure induction plasma generation. Comparison of rf power (a), and dc-rf power conversion efficiency (b).

6. Conclusions

A novel T-LCL type immittance circuit is designed in the high-frequency (MHz) range for constant-current high-power operation to enhance the power efficiency, thereby generating high-pressure radio-frequency inductive discharges in near atmospheric pressure efficiently. Although it is difficult to design an ideal immittance circuit for inductive plasma load due to the presence of residual resistance in the reactive components, the result reported in this article using the designed immittance circuit shows comprehensive improvements over the conventional series resonance circuit. The experimental results shows that the immittance circuit confirms injecting higher effective rf power into the plasma, thereby enhancing the dc-rf conversion efficiency as well as the plasma heating efficiency (with a relatively high rf power) as much as three times than that of the series resonance circuit, and assists to generate efficient rf inductive discharges with up to one atmosphere in argon.

Acknowledgements

The authors would like to thanks to Mr. Takagi for his technical assistance during the experimental setup.

References

- [1] W. Hittorf, *Wiedsmann Ann. D. Physik.* **21**, 90 (1884).
- [2] T.B. Reed, *J. Appl. Phys.* **32**, 821 (1961).
- [3] T.B. Reed, *J. Appl. Phys.* **32**, 2534 (1961).
- [4] A. Merkhof and M.I. Boulos, *Plasma Sources Sci. Technol.* **7**, 599 (1998).
- [5] Y. Tanaka and T. Sakuta, *J. Phys. D: Appl. Phys.* **35**, 468 (2002).
- [6] A.B. Murphy, *J. Phys. D: Appl. Phys.* **34**, R151 (2001).
- [7] V.A. Godyak, R.B. Piejak and B. M. Alexandrovich, *J.*

- Appl. Phys. **85**, 703 (1999).
- [8] C.W. Chung, S.H. Seo and H.Y. Chang, Phys. Plasmas **7**, 3584 (2000).
- [9] A. Smolyakov, V. Godyak and A. Duffy, Phys. Plasmas **7**, 4755 (2000).
- [10] S. Xu, K.N. Ostrokov, Y. Li, E.L. Tsakadze and I.R. Jones, Phys. Plasmas **8**, 2549 (2001).
- [11] J Reece Roth, *Industrial Plasma Engineering-Volume 1: Principles* (Institute of Physics Publishing, Bristol, 1995).
- [12] S. Watanabe, Y. Uesugi, S. Ohsawa and S. Takamura, Rev. Sci. Inst. **69**, 355 (1998).
- [13] T. Yoshida, T. Tani, H. Nishimura and K. Akashi, J. Appl. Phys. **54**, 640 (1983).
- [14] T. Uesugi, O. Nakamura, T. Yoshida and K. Akashi, J. Appl. Phys. **64**, 3874 (1988).
- [15] M.A. Razzak, K. Kondo, Y. Uesugi, and S. Takamura, *Annual Meeting of the Fundamentals and Materials Society of IEE Japan*, Tokyo 112 (2002).
- [16] J Reece Roth, *Industrial Plasma Engineering-Volume 2: Applications to Nonthermal Plasma Processing* (Institute of Physics Publishing, Bristol, 2001).
- [17] M. I Boulos, P. Fauchais and E. Phender, *Thermal Plasmas: Fundamentals and Applications* (Plenum press, New York, 1994).
- [18] Y. Uesugi, T. Adachi, K. Kondo and S. Takamura, Trans. IEE Japan **122A**, 461 (2002) [in Japanese].
- [19] H. Oguchi, R. Shimotaya, T. Shimizu, H. Takagi and M. Ito, Trans. IEE Japan **121D**, 805 (2001).
- [20] M.A. Razzak, K. Kondo, Y. Uesugi, N. Ohno and S. Takamura, J. Appl. Phys. **95**, 427 (2004).
- [21] M.A. Razzak, S. Takamura and Y. Uesugi, J. Appl. Phys. **96**, 4771 (2004).
- [22] M.A. Razzak, H. Ukai, Y. Uesugi and S. Takamura, *International COE forum on Plasma Science and Technology*, Nagoya 83 (2004).
- [23] M.A. Razzak, Y. Suzuki, S. Takamura and Y. Uesugi, *The XVth International Conference on Gas Discharges and Their Applications*, Toulouse 505 (2004).